

Constrained exceptional supersymmetric standard model with a Higgs signal near 125 GeVP. Athron,^{1,*} S. F. King,^{2,†} D. J. Miller,^{3,‡} S. Moretti,^{2,§} and R. Nevzorov^{4,||,¶}¹*ARC Centre of Excellence for Particle Physics at the Terascale, School of Chemistry and Physics, The University of Adelaide, Adelaide, SA 5005, Australia*²*School of Physics and Astronomy, University of Southampton, Southampton, SO17 1BJ, United Kingdom*³*SUPA, School of Physics and Astronomy, University of Glasgow, Glasgow, G12 8QQ, United Kingdom*⁴*Department of Physics and Astronomy, University of Hawaii, Honolulu, Hawaii 96822, USA*

(Received 7 September 2012; published 1 November 2012)

We study the parameter space of the constrained exceptional supersymmetric standard model (cE₆SSM) consistent with a Higgs signal near 125 GeV and the LHC searches for squarks, gluinos and Z'. The cE₆SSM parameter space, consistent with correct electroweak symmetry breaking, is represented by scans in the (m₀, M_{1/2}) plane for fixed Z' mass and tanβ, with squark, gluino and Higgs masses plotted as contours in this plane. We find that a 125 GeV Higgs mass only arises for a sufficiently large Z' mass, mostly above current limits, and for particular regions of squark and gluino masses corresponding to multi-TeV squark masses, but with lighter gluinos typically within reach of the LHC 8 TeV or forthcoming 14 TeV runs. Successful dark matter relic abundance may be achieved over all the parameter space, assuming a binolike lightest supersymmetric particle with a nearby heavier inert Higgsino doublet and decoupled inert singlinos, resulting in conventional gluino decay signatures. A set of typical benchmark points with a Higgs near 125 GeV is provided which exemplifies these features.

DOI: [10.1103/PhysRevD.86.095003](https://doi.org/10.1103/PhysRevD.86.095003)

PACS numbers: 12.60.Jv

I. INTRODUCTION

The ATLAS and CMS Collaborations have recently presented the first indication for a Higgs boson with a mass about 125 GeV, consistent with the allowed window of Higgs masses 125 ± 3 GeV [1,2]. In general, these results have generated much excitement in the community, and already there are a number of papers discussing the implications of such a Higgs boson [3]. Many of these studies focus on the possibility that the Higgs boson arises from a supersymmetric standard model (SSM). However there are several SSMs which are capable of giving rise to a SM-like Higgs boson and it is interesting to survey some leading possibilities.

In the minimal supersymmetric standard model (MSSM) the lightest Higgs boson is lighter than about 130–135 GeV, depending on top squark parameters (see e.g., Ref. [4] and references therein). A 125 GeV SM-like Higgs boson is consistent with the MSSM in the decoupling limit. In the limit of decoupling the light Higgs mass is given by

$$m_h^2 \approx M_Z^2 \cos^2 2\beta + \Delta m_h^2, \quad (1)$$

where Δm_h^2 is dominated by loops of heavy top quarks and top squarks and tanβ is the ratio of the vacuum expectation values (VEVs) of the two Higgs doublets introduced in the

MSSM Higgs sector. At large tanβ, we require $\Delta m_h \approx 85$ GeV which means that a very substantial loop contribution, nearly as large as the tree-level mass, is needed to raise the Higgs boson mass to 125 GeV.

In the next-to-minimal supersymmetric standard model (NMSSM), the spectrum of the MSSM is extended by one singlet superfield [5–7] (for reviews see Ref. [8]). In the NMSSM the supersymmetric Higgs mass parameter μ is promoted to a gauge-singlet superfield, S, with a coupling to the Higgs doublets, λSH_uH_d, that is perturbative up to unified scales. In the pure NMSSM values of λ ~ 0.7 do not spoil the validity of perturbation theory up to the grand unified theory (GUT) scale only providing tanβ ≥ 4; however the presence of additional extra matter allows smaller values of tanβ to be achieved [9]. The maximum mass of the lightest Higgs boson in the NMSSM is

$$m_h^2 \approx M_Z^2 \cos^2 2\beta + \lambda^2 v^2 \sin^2 2\beta + \Delta m_h^2, \quad (2)$$

where here we use v = 174 GeV. For λv > M_Z, the tree-level contributions to m_h are maximized for moderate values of tanβ rather than by large values of tanβ as in the MSSM. For example, taking λ = 0.7 and tanβ = 2, these tree-level contributions raise the Higgs boson mass to about 112 GeV, and Δm_h ≥ 55 GeV is required. This is to be compared to the MSSM requirement Δm_h ≥ 85 GeV. The difference between these two values (numerically about 30 GeV) is significant since Δm_h depends logarithmically on the stop masses as well as receiving an important contribution from stop mixing. This means for example that, unlike the MSSM, in the case of the NMSSM maximal stop mixing is not required to get the Higgs heavy enough.

*peter.athron@adelaide.edu.au

†king@soton.ac.uk

‡david.j.miller@glasgow.ac.uk

§stefano@phys.soton.ac.uk

||nevezorov@phys.hawaii.edu

¶On leave of absence from the Theory Department, ITEP, Moscow, Russia.

In the exceptional supersymmetric standard model (E_6 SSM) [10,11], the spectrum of the MSSM is extended to fill out three complete 27-dimensional representations of the gauge group E_6 which is broken at the unification scale down to the SM gauge group plus one additional gauged $U(1)_N$ symmetry at low energies under which right-handed neutrinos are neutral, allowing them to get large masses. Each 27-plet contains one generation of ordinary matter; singlet fields, S_i ; up and down type Higgs doublets, $H_{u,i}$ and $H_{d,i}$; and charged $\pm 1/3$ colored exotics D_i, \bar{D}_i . The extra matter ensures anomaly cancellation; however the model also contains two extra $SU(2)$ doublets, H' and \bar{H}' , which are required for gauge coupling unification [12]. To evade rapid proton decay either a Z_2^B or Z_2^L symmetry is introduced and to evade large flavor changing neutral currents an approximate Z_2^H symmetry is introduced which ensures that only the third family of Higgs $H_{u,3}$ and $H_{d,3}$ couple to fermions and get VEVs. Similarly only the third family singlet S_3 gets a VEV, $\langle S_3 \rangle = s/\sqrt{2}$, which is responsible for the effective μ term and D -fermion mass. The first and second families of Higgs and singlets which do not get VEVs are called “inert.” The maximum mass of the lightest SM-like Higgs boson in the E_6 SSM is [10]

$$m_h^2 \approx M_Z^2 \cos^2 2\beta + \lambda^2 v^2 \sin^2 2\beta + \frac{M_Z^2}{4} \left(1 + \frac{1}{4} \cos 2\beta \right)^2 + \Delta m_h^2, \quad (3)$$

where the extra contribution relative to the NMSSM value in Eq. (2) is due to the $U(1)_N$ D term. The Higgs mass can be larger due to two separate reasons: firstly the value of λ may be larger due to the extra matter, and secondly due to the $U(1)_N$ D -term contribution equal to $\frac{1}{2} M_Z (\frac{3}{8} M_Z)$ GeV for low (high) $\tan\beta$. For example for large $\tan\beta$, where the NMSSM term $\lambda^2 v^2 \sin^2 2\beta$ is unimportant, the E_6 SSM requires $\Delta m_h \approx 78$ GeV as compared to $\Delta m_h \approx 85$ GeV in the MSSM.

In a previous paper we considered a constrained version of the E_6 SSM with universal gaugino mass $M_{1/2}$, soft scalar mass m_0 , and soft trilinear mass A at the unification scale M_X [13]. Previous studies of the constrained exceptional supersymmetric standard model (c E_6 SSM) have focused on regions of c E_6 SSM parameter space which could have led to a discovery with the first LHC data [14] via the characteristic LHC signatures of the model [15]. These “early” benchmark points are by now excluded by LHC searches for supersymmetry (SUSY) and Z' bosons. The main purpose of the present paper is to consider the c E_6 SSM in the light of the Higgs signal near 125 GeV, taking into account the latest LHC constraints on squarks, gluinos and Z' following the 7 TeV run. We find that there are huge unexplored regions of parameter space in the c E_6 SSM which are consistent with a SM-like Higgs boson with a mass in the allowed window 125 ± 3 GeV. The c E_6 SSM parameter space, consistent with correct electroweak symmetry

breaking, is represented here by scans in the $(m_0, M_{1/2})$ plane for fixed Z' mass and $\tan\beta$, with squark, gluino and Higgs masses plotted as contours in this plane. If the Higgs mass is determined accurately then this will narrow down the preferred regions of parameter space considerably. For example, we find that a 125 GeV Higgs mass only arises for a sufficiently large Z' mass, mostly above current limits, and for particular regions of squark and gluino masses corresponding to multi-TeV squark masses, but with lighter gluinos typically within reach of forthcoming LHC 8 TeV or 14 TeV runs. Successful dark matter relic abundance may be achieved over all the parameter space, assuming a binolike lightest supersymmetric particle (LSP) with a nearby heavier inert Higgsino doublet and decoupled inert singlinos, resulting in conventional gluino decay signatures. A set of typical benchmark points with a Higgs near 125 GeV is provided which exemplifies these features and demonstrates the huge unexplored range of parameter space in this model with multi-TeV Z' and squark masses but with lighter gluinos, winos and binos, as well as possibly light colored exotic D fermions.

The layout of the rest of the paper is as follows. In Sec. II we review the c E_6 SSM. In Sec. III we discuss existing LHC constraints arising from Higgs searches, sparticle searches, exotica searches and Z' searches. In Sec. IV we show that successful dark matter relic abundance may be achieved over all the parameter space, assuming a binolike LSP with a nearby heavier inert Higgsino doublet and decoupled inert singlinos, resulting in conventional gluino decay signatures. In Sec. V we provide detailed scans of the parameter space in the c E_6 SSM, presenting the results in the $(m_0, M_{1/2})$ plane for fixed Z' mass and $\tan\beta$, with squark, gluino and Higgs masses plotted as contours in this plane. We also present new heavy benchmarks for the model and discuss their phenomenology. Section VI concludes the paper.

II. c E_6 SSM

The E_6 SSM is a supersymmetric model based on the $SU(3)_C \times SU(2)_W \times U(1)_Y \times U(1)_N$ gauge group which is a subgroup of E_6 . The extra $U(1)_N$ symmetry is the combination $U(1)_\chi \cos\theta + U(1)_\psi \sin\theta$ with $\theta = \arctan\sqrt{15}$. In order to ensure anomaly cancellation the particle content of the E_6 SSM is extended to include three complete fundamental 27 representations of E_6 . In addition the low energy particle spectrum of the E_6 SSM is supplemented by $SU(2)_W$ doublet H' and antidoublet \bar{H}' states from the extra $27'$ and $\bar{27}'$ to preserve gauge coupling unification. These components of the E_6 fundamental representation originate from $(5^*, 2)$ of $27'$ and $(5, -2)$ of $\bar{27}'$ by construction. The analysis performed in Ref. [12] shows that the unification of gauge couplings in the E_6 SSM can be achieved for any phenomenologically acceptable value of $\alpha_3(M_Z)$ consistent with the measured low energy central value, unlike in the MSSM which, ignoring the effects of high energy

threshold corrections, requires significantly higher values of $\alpha_3(M_Z)$, well above the experimentally measured central value. Because supermultiplets H' and \bar{H}' have opposite $U(1)_Y$ and $U(1)_N$ charges their contributions to the anomalies are canceled identically.

Thus, in addition to a Z' associated with the $U(1)_N$ symmetry, the E_6 SSM involves extra matter beyond the MSSM with the quantum numbers of three $5 + 5^*$ representations of $SU(5)$ plus three $SU(5)$ singlets with $U(1)_N$ charges. The matter content of the E_6 SSM with correctly normalized Abelian charges of all matter fields is summarized in Table I. The presence of a Z' boson and exotic quarks predicted by the E_6 SSM provides spectacular new physics signals at the LHC which were discussed in Refs. [10,11,13–16].

Since right-handed neutrinos N^c do not participate in gauge interactions they are expected to gain masses at some intermediate scale after the breakdown of E_6 [10,17] while the remaining matter survives down to the low energy scale near which the gauge group $U(1)_N$ is broken. The heavy right-handed neutrinos shed light on the origin of the mass hierarchy in the lepton sector allowing them to be used for the seesaw mechanism. At the same time the heavy Majorana right-handed neutrinos may decay into final states with lepton number $L = \pm 1$, thereby creating a lepton asymmetry in the early Universe. Since in the E_6 SSM the Yukawa couplings of the new exotic particles are not constrained by neutrino oscillation data, substantial values of the charge conjugation and parity (CP) asymmetries can be induced even for a relatively small mass of the lightest right-handed neutrino ($M_1 \sim 10^6$ GeV) so that successful thermal leptogenesis may be achieved without encountering a gravitino problem [18].

Although the presence of TeV scale exotic matter in E_6 SSM gives rise to spectacular collider signatures, it also leads to nondiagonal flavor transitions and rapid proton decay. To suppress flavor changing processes as well as baryon and lepton number violating operators one can postulate a Z_2^H symmetry, under which all superfields except one pair of $H_{d,i}$ and $H_{u,i}$ (say $H_d \equiv H_{d,3}$ and $H_u \equiv H_{u,3}$) and one SM-type singlet superfield ($S \equiv S_3$) are odd [10,11]. Here we also impose a discrete Z_2^S symmetry, under which only first and second generation singlet superfields are odd, i.e., $S_{1,2} \rightarrow -S_{1,2}$, whereas all other supermultiplets are even [19]. In this case the fermionic components of S_1 and S_2 essentially decouple from the rest of the spectrum and the lightest neutralino

may be absolutely stable and can play the role of dark matter. The Z_2^H and Z_2^S symmetries reduce the structure of the Yukawa interactions to simplify the form of the E_6 SSM superpotential substantially. Integrating out heavy Majorana right-handed neutrinos and keeping only Yukawa interactions whose couplings are allowed to be of order unity leaves us with the following phenomenologically viable superpotential:

$$\begin{aligned}
 W_{E_6SSM} \simeq & \lambda S(H_d H_u) + \lambda_\alpha S(H_{d,\alpha} H_{u,\alpha}) + \kappa_i S(D_i \bar{D}_i) \\
 & + h_i(H_u Q)t^c + h_b(H_d Q)b^c + h_\tau(H_d L)\tau^c \\
 & + \mu'(H' \bar{H}') + h_{4j}^E(H_d H')e_j^c,
 \end{aligned} \quad (4)$$

where $\alpha = 1, 2$ and $i = 1, 2, 3$, and where the superfields $L = L_3$, $Q = Q_3$, $t^c = u_3^c$, $b^c = d_3^c$ and $\tau^c = e_3^c$ belong to the third generation and λ_i , κ_i are dimensionless Yukawa couplings with $\lambda \equiv \lambda_3$. In Eq. (4) we choose the basis $H_{d,\alpha}$, $H_{u,\alpha}$, D_i and \bar{D}_i so that the Yukawa couplings of the singlet field S have flavor diagonal structure. Hereafter, we assume that the couplings h_{4j}^E are rather small and can be neglected.

From Eq. (4) it follows that the $SU(2)_W$ doublets H_u and H_d , that are even under the Z_2^H symmetry, play the role of Higgs fields generating the masses of quarks and leptons through electroweak (EW) symmetry breaking (EWSB) while the other generations of these Higgs-like fields remain inert. The singlet field S must also acquire a large VEV in order to induce sufficiently large masses for the exotic charged fermions and Z' boson. The couplings λ_i and κ_i should be large enough to ensure that the exotic fermions are sufficiently heavy to avoid conflict with direct particle searches at present and former accelerators. If λ_i or κ_i are reasonably large they affect the evolution of the soft scalar mass m_S^2 of the singlet field S rather strongly, resulting in negative values of m_S^2 at low energies that trigger the breakdown of the $U(1)_N$ symmetry.

Initially the sector of EWSB in the E_6 SSM involves ten degrees of freedom. However four of them are massless Goldstone modes which are swallowed by the W^\pm , Z and Z' gauge bosons that gain nonzero masses. If CP invariance is preserved the other degrees of freedom form two charged, one CP -odd and three CP -even Higgs states. When the SUSY breaking scale is considerably larger than the EW scale, the mass matrix of the CP -even Higgs sector has a hierarchical structure and can be diagonalized using perturbation theory [7,20]. In this case the mass of one CP -even Higgs particle is always close to the Z' boson mass $M_{Z'}$. The masses of another

TABLE I. The $U(1)_Y$ and $U(1)_N$ charges of matter fields in the E_6 SSM, where Q_i^N and Q_i^Y are here defined with the correct E_6 normalization factor required for the RG analysis.

	Q	u^c	d^c	L	e^c	N^c	S	H_2	H_1	D	\bar{D}	H'	\bar{H}'
$\sqrt{\frac{2}{3}}Q_i^Y$	$\frac{1}{6}$	$-\frac{2}{3}$	$\frac{1}{3}$	$-\frac{1}{2}$	1	0	0	$\frac{1}{2}$	$-\frac{1}{2}$	$-\frac{1}{3}$	$\frac{1}{3}$	$-\frac{1}{2}$	$\frac{1}{2}$
$\sqrt{40}Q_i^N$	1	1	2	2	1	0	5	-2	-3	-2	-3	2	-2

CP -even, the CP -odd and the charged Higgs states are almost degenerate. When $\lambda \gtrsim g'_1$, the qualitative pattern of the Higgs spectrum is rather similar to the one which arises in the Peccei Quinn symmetric NMSSM [7,21]. In the considered limit the heaviest CP -even, CP -odd and charged states are almost degenerate and lie beyond the TeV range [10]. Finally, like in the MSSM and NMSSM, one of the CP -even Higgs bosons is always light irrespective of the SUSY breaking scale. However, in contrast with the MSSM, the lightest Higgs boson in the E_6 SSM can be heavier than 110–120 GeV even at tree level. In the two-loop approximation the lightest Higgs boson mass does not exceed 150–155 GeV [10]. In our analysis here we explore the part of the parameter space of the constrained E_6 SSM which is associated with the SM-like Higgs boson mass around 125 GeV.

Although Z_2^H eliminates problems related with baryon number violation and nondiagonal flavor transitions it also forbids all interactions that allow the lightest exotic quarks to decay. Since models with stable charged exotic particles are ruled out by experiment [22] the Z_2^H symmetry can only be approximate. The appropriate suppression of the proton decay rate can be achieved if one imposes either a Z_2^L or a Z_2^B discrete symmetry [10]. If the Lagrangian is invariant with respect to a Z_2^L symmetry, under which all superfields except lepton ones are even (Model I), then the terms in the superpotential which permit the lightest exotic quarks to decay and are allowed by the gauge symmetry can be written as follows:

$$W_1 = g_{ijk}^O D_i(Q_j Q_k) + g_{ijk}^q \bar{D}_i d_j^c u_k^c. \quad (5)$$

In this case the baryon number conservation requires exotic quarks to be diquarks. The invariance of the Lagrangian with respect to Z_2^B symmetry (Model II), under which supermultiples $H_i^d, H_i^u, S_i, Q_i, u_i^c, d_i^c$ are even while the exotic quark (D_i and \bar{D}_i) as well as lepton superfields (L_i, e_i^c, N_i^c) are odd, implies that the following couplings are allowed:

$$W_2 = g_{ijk}^E e_i^c D_j u_k^c + g_{ijk}^D (Q_i L_j) \bar{D}_k. \quad (6)$$

As a consequence, in Model II, \bar{D}_i and D_i manifest themselves in the Yukawa interactions as leptoquarks. With both of these symmetries the MSSM particle content behaves like it does under R parity, with the subset of particles present in the standard model and Higgs (and also inert Higgs) bosons being even under this generalized R parity, while their supersymmetric partners are odd and therefore, as usual, must be pair produced, and upon decaying will always give rise to a stable LSP. However the exotic D fermions are odd and so must be pair produced and will decay into a LSP, while their scalar superpartners are even and in some cases can be singly produced.

In both models discussed above the Z_2^H symmetry violating couplings are not forbidden. Nevertheless because the Z_2^H symmetry violating operators lead to nondiagonal

flavor interactions, the corresponding Yukawa couplings are expected to be small, and must preserve either the Z_2^B or Z_2^L symmetry to ensure proton stability. In particular, to suppress flavor changing processes the Yukawa couplings of the inert Higgs states to the quarks and leptons of the first two generations should be smaller than $10^{-3} - 10^{-4}$. In our analysis small Z_2^H symmetry violating couplings can be ignored in the first approximation.

Assuming that $h_{4j}^E \rightarrow 0$ the superpotential of the E_6 SSM which is invariant with respect to both Z_2^H and Z_2^S symmetries involves only six extra Yukawa couplings (λ_i and κ_i) as compared with the MSSM with $\mu = 0$. The soft breakdown of SUSY gives rise to many new parameters. For instance, it induces additional trilinear scalar couplings associated with the Yukawa interactions as well as a set of soft scalar masses. The number of fundamental parameters reduces drastically within a constrained version of the model (c E_6 SSM) [13,14], defined at the GUT scale M_X , where all gauge couplings coincide, i.e., $g_1(M_X) \simeq g_2(M_X) \simeq g_3(M_X) \simeq g'_1(M_X)$. Constrained SUSY models imply that all soft scalar masses are set to be equal to m_0 at some high energy scale M_X , all gaugino masses $M_i(M_X)$ are equal to $M_{1/2}$ and trilinear scalar couplings are such that $A_i(M_X) = A_0$. Thus the c E_6 SSM is characterized by the following set of Yukawa couplings and universal soft SUSY breaking terms:

$$\lambda_i(M_X), \quad \kappa_i(M_X), \quad h_t(M_X), \quad h_b(M_X), \quad h_\tau(M_X), \\ m_0, \quad M_{1/2}, \quad A_0, \quad (7)$$

where $h_t(M_X)$, $h_b(M_X)$ and $h_\tau(M_X)$ are the usual t -quark, b -quark and τ -lepton Yukawa couplings, and $\lambda_i(M_X)$, $\kappa_i(M_X)$ are the extra Yukawa couplings defined in Eq. (7). Near the GUT scale M_X the part of the scalar potential V_{soft} that contains a set of the soft SUSY breaking terms takes the form

$$V_{\text{soft}} = m_0^2 27_i 27_i^* + A_0 Y_{ijk} 27_i 27_j 27_k + \text{H.c.}, \quad (8)$$

where Y_{ijk} are generic Yukawa couplings from the trilinear terms in Eq. (4) and the 27_i represent generic fields from Table I and in particular those which appear in Eq. (4). Since Z_2^H and Z_2^S symmetries forbid many terms in the superpotential of the E_6 SSM it also forbids similar soft SUSY breaking terms in V_{soft} . In order to guarantee correct EWSB, m_0^2 has to be positive. To simplify our analysis we also assume that A_0 is real and $M_{1/2}$ is positive—this then naturally leads to real VEVs of the Higgs fields.

The set of c E_6 SSM parameters in Eq. (7) should in principle be supplemented by μ' and the associated bilinear scalar coupling B' . The term $\mu'(H'\bar{H}')$ is the only bilinear term in the superpotential Eq. (4). It is solely responsible for the masses of the charged and neutral components of H' and \bar{H}' . The corresponding mass term is not suppressed by E_6 symmetry and is not involved in the process of EWSB. Therefore the parameter μ' remains

arbitrary. Recent analysis revealed that the gauge coupling unification in the E_6 SSM is consistent with μ' around 100 TeV [12]. Therefore we assume that the parameter μ' can be as large as 10 TeV so that the scalar and fermion components of the superfields H' and \bar{H}' are very heavy. As a result they decouple from the rest of the particle spectrum and the parameters B' and μ' are irrelevant for our analysis. This also justifies why the Yukawa couplings h_{4j}^E can be neglected in the first approximation if they are not too large.

To calculate the particle spectrum within the cE_6 SSM one must find sets of parameters which are consistent with both the high scale universality constraints and the low scale EWSB constraints. To evolve between these two scales we use two-loop renormalization group equations (RGEs) for the gauge and Yukawa couplings together with two-loop RGEs for $M_a(Q)$ and $A_i(Q)$ as well as one-loop RGEs for $m_i^2(Q)$. The low energy values of the soft SUSY breaking terms can be determined semianalytically as functions of A_0 , $M_{1/2}$ and m_0 . The corresponding semi-analytic expressions can be written as

$$\begin{aligned} m_i^2(Q) &= a_i(Q)M_{1/2}^2 + b_i(Q)A_0^2 + c_i(Q)A_0M_{1/2} + d_i(Q)m_0^2, \\ A_i(Q) &= e_i(Q)A_0 + f_i(Q)M_{1/2}, \\ M_i(Q) &= p_i(Q)A_0 + q_i(Q)M_{1/2}, \end{aligned} \quad (9)$$

where Q is the renormalization scale. The analytic expressions for the coefficients $a_i(Q)$, $b_i(Q)$, $c_i(Q)$, $d_i(Q)$, $e_i(Q)$, $f_i(Q)$, $p_i(Q)$, $q_i(Q)$ are unknown, since an exact analytic solution of the E_6 SSM RGEs is not available. Nevertheless these coefficients may be calculated numerically at the low energy scale. We use semianalytic expressions Eq. (9) in our analysis to determine the sets of m_0 , $M_{1/2}$ and A_0 which are consistent with EWSB. This allows one to replace m_0 , $M_{1/2}$ and A_0 by ν , $\tan\beta$ and s through the EWSB conditions, in a similar manner to the way $|\mu|$ and B are traded for $\tan\beta$ and ν in the MSSM. This means that the particle spectrum and other phenomenological aspects of the model are defined by only eight free parameters, which in previous analyses have been taken to be $\{\lambda_i, \kappa_i, s, \tan\beta\}$ ¹ and can be reduced further by considering scenarios with some Yukawa coupling universality or other well motivated relations between the Yukawa couplings at the GUT scale.

Although correct EWSB is not guaranteed in the cE_6 SSM, remarkably, there are always solutions with real A_0 , $M_{1/2}$ and m_0 for sufficiently large values of κ_i , which drive m_S^2 negative. This is easy to understand since the κ_i couple the singlet to a large multiplicity of colored fields, thereby efficiently driving its squared mass negative to trigger the breakdown of the gauge symmetry.

To calculate the particle spectrum within the cE_6 SSM a private spectrum generator has been written, based on some routines and the class structure of SOFTSUSY 2.0.5 [23].

¹This should be compared to the c MSSM with $\{m_0, M_{1/2}, A, \tan\beta, \text{sign}(\mu)\}$.

The details of the procedure we followed, including the RGEs for the E_6 SSM and the experimental and theoretical constraints can be found in Ref. [13,14]. To avoid any conflict with collider experiments as well as with recent cosmological observations we impose the set of constraints specified in the next section. These bounds restrict the allowed range of the parameter space in the cE_6 SSM.

III. LHC CONSTRAINTS

A. Higgs searches

At present, the situation in ATLAS on Higgs mass limits within the SM hypothesis is well summarized in Ref. [1]. Herein, a preliminary combination of SM Higgs boson searches was performed in a data set corresponding to an integrated luminosity of 4.6 to 4.9 fb^{-1} taken at 7 TeV. A SM Higgs boson is excluded at the 95% CL in the mass ranges 110.0–117.5 GeV, 118.5–122.5 GeV and 129–539 GeV, while the range 120–555 GeV is expected to be excluded in the absence of a signal. The mass regions between 130 and 486 GeV are excluded at the 99% C.L. An excess of events is observed around 126 GeV with a local significance of 2.5σ , where the expected significance in the presence of a SM Higgs boson for that mass hypothesis is 2.9σ .

Combined results were reported by CMS in Ref. [2], based on searches for the SM Higgs boson at 7 TeV in the usual five decay modes: $\gamma\gamma$, $b\bar{b}$, $\tau^+\tau^-$, WW and ZZ . The explored Higgs boson mass range is 110–600 GeV. The analyzed data correspond to an integrated luminosity of 4.6–4.8 fb^{-1} . The expected excluded mass range in the absence of the SM Higgs boson is 118–543 GeV at 95% C.L. The observed results exclude the SM Higgs boson in the mass range 127–600 GeV at 95% C.L. and in the mass range 129–525 GeV at 99% C.L. An excess of events above the expected SM background is observed at the low end of the explored mass range making the observed limits weaker than expected in the absence of a signal. The largest excess, with a local significance of 3.1σ , is observed for a SM Higgs boson mass hypothesis of 124 GeV.

All our benchmarks presume the lightest Higgs boson mass in the tentative signal range of 124–126 GeV. Further, by making use of a modification of the programs described in Refs. [24,25], we have checked that the cross section times branching ratio (BR) rates for the process $pp \rightarrow h_1 \rightarrow X$, where X represents the aforementioned channels in which ATLAS and CMS have shown sensitivity to a Higgs boson with such a mass, as obtained in the cE_6 SSM, differ by no more than 7–8% from those of the SM. In particular, notice that we have allowed in the case of the cE_6 SSM also for all possible non-SM states belonging to its spectrum that could enter the $gg \rightarrow h_1$ loop diagram at production level and the $h_1 \rightarrow gg$, $\gamma\gamma$, $Z\gamma$ loop diagrams at decay level. Masses of the SM states were the same in both calculations, while the relevant gauge couplings were

different, as extracted from the corresponding RGEs of the two models.

B. Sparticle searches

Recent searches for supersymmetry by both ATLAS and CMS have considerably reduced the available parameter space for low energy supersymmetric models. Of particular interest are searches for squarks of the first two generations and gluinos, which have been probed by ATLAS using final states with jets and missing transverse momentum and possibly an isolated lepton [26–28], all performed with 4.7 fb^{-1} of data. Similarly, the CMS collaboration has provided interesting exclusions by forcing events with missing transverse energy into a dijet topology [29] using 4.4 fb^{-1} of data, or alternatively by using the M_{T2} variable [30] on 4.73 fb^{-1} of data.

These exclusions are, of course, sensitive to the details of the supersymmetric model. Both ATLAS and CMS chose to interpret their searches as exclusions in the m_0 – $M_{1/2}$ plane of the cMSSM fixing values for the other cMSSM parameters $\tan\beta$, A_0 and the sign of μ . For our purposes, these exclusions must be reinterpreted for the cE₆SSM. This presents two difficulties. First of all, the m_0 and $M_{1/2}$ values of the cMSSM bear little relation to their counterparts in the cE₆SSM; the RGE running from the unification scale results in a completely different low energy spectrum, so a particular choice of m_0 and $M_{1/2}$ will yield different squark and gluino masses in each model. This is further exacerbated by the arbitrary choice of parameters $\tan\beta$, A_0 and the sign of μ , which will not, in general, correspond to the parameter choices for the cE₆SSM. Fortunately, both CMS and ATLAS have also superimposed contours of squark and gluino masses on their exclusion plots. These contours tell us that for reasonably heavy squarks, above about 1.5 TeV, we must ensure that our gluinos are heavier than about 850 GeV or so.

The “about” and “or so” of the last sentence are a product of our second difficulty: the squarks and gluinos must necessarily decay to lighter supersymmetric states in the spectrum, including the LSP. As already pointed out, the m_0 and $M_{1/2}$ used to determine the (cMSSM) experimental exclusions may predict a rather different spectrum for the cE₆SSM scenario with analogous squark and gluino masses. Therefore the cE₆SSM squarks and gluinos may have decay widths and branching ratios considerably different from those used for the experimental exclusion. It has been pointed out in Ref. [31] that supersymmetry with a *compressed* spectrum, that is with smaller mass intervals between the particle states, may avoid experimental exclusions since the decays may contain less missing momentum.

Without a dedicated experimental analysis of the E₆SSM we are unable to determine how the experimental limits on squarks and gluinos will be changed by these effects. Consequently we will adopt a conservative approach and insist that our benchmark scenarios are considerably

beyond these limits—namely that our first and second generation squarks are significantly heavier than 1.4 TeV and our gluinos are significantly heavier than 850 GeV.

Searches for the third generation squarks by ATLAS are less well developed and, as yet, only available for the 2.1 fb^{-1} data set. A search for bottom squarks in the MSSM, assuming a 100% branching ratio for the decay $\tilde{b}_1 \rightarrow b\tilde{\chi}_1^0$, excludes bottom squark masses up to 390 GeV for neutralino masses below 60 GeV [32]. Top squark constraints are also rather weak, with an exclusion of top squark masses below 310 GeV as long as the neutralino is in the mass window 115–230 GeV [33]. This study assumed a gauge mediated supersymmetry breaking model.

CMS has also produced an exclusion in the plane of the gluino and LSP masses for a simplified model [30,34] using the process $pp \rightarrow \tilde{g}\tilde{g}$ with $\tilde{g} \rightarrow b\tilde{\chi}_1^0$ and 4.73 fb^{-1} (also see Ref. [35]). For gluino masses below about 1 TeV, this analysis excludes a lightest neutralino lighter than about 440 GeV, with this limit reducing quickly for higher gluino masses, disappearing entirely by 1.06 TeV. However, this simplified model requires a rather specific spectrum, and it is not clear how applicable this is to our cE₆SSM case.

One final analysis of note is an ATLAS search for direct neutralino and chargino production in a simplified model where the lightest chargino and next-to-lightest neutralino are degenerate [36]. Using 2.06 fb^{-1} of data, this study concluded that these degenerate $\tilde{\chi}_1^\pm/\tilde{\chi}_2^0$ are excluded up to 300 GeV for a lightest neutralino lighter than 250 GeV.

C. Exotica searches

The production of TeV scale exotic colored states should also lead to spectacular LHC signals. Several experiments at LEP, HERA, Tevatron and LHC were searching for the colored objects that decay into either a pair of quarks or a quark and a lepton. But most searches imply that exotic color states, i.e., leptoquarks or diquarks, have integer—spin. So they are either scalars or vectors. Because of this, new colored objects can be coupled directly to either a pair of quarks or to a quark and a lepton. Moreover it is usually assumed that leptoquarks and diquarks have appreciable couplings to the quarks and leptons of the first generation. The most stringent constraints on the masses of leptoquarks come from the nonobservation of these exotic color states at the ATLAS experiment. Recently ATLAS Collaboration ruled out first and second generation scalar leptoquarks (i.e., leptoquarks that couple to the first and second generation fermions respectively) with masses below 320–420 GeV [37]. The experimental lower bounds on the masses of diquarks (dijet resonances) tend to be considerably higher (see, for example, Ref. [38]).

However the LHC lower bounds on the masses of exotic colored states mentioned above are not directly applicable in the case of the E₆SSM (also see Ref. [39]). Indeed, our analysis of the particle spectrum within cE₆SSM indicates

that \tilde{D} scalars tend to be rather heavy. On the other hand exotic D fermions can have masses below the TeV scale. Assuming that they couple most strongly to the third family (s)quarks and (s)leptons, the lightest exotic D fermions decay into $\tilde{t}b$, $\tilde{t}\tilde{b}$, $\tilde{t}\tilde{b}$ (if they are diquarks) or $\tilde{t}\tau$, $\tilde{t}\tilde{\tau}$, $\tilde{b}\nu_\tau$, $\tilde{b}\tilde{\nu}_\tau$ (if they are leptoquarks) resulting in the missing energy and transverse momentum in the final state. This is because these states are odd under the analogue of R parity in the E_6 SSM. Due to the presence of missing energy in the final states of the decays of D fermions a special dedicated study is required to determine the experimental limits on their masses and couplings.

D. Z' searches

Recent 95% C.L. mass limits on Z' bosons of E_6 origin (in dilepton searches) from ATLAS based on 5 fb^{-1} of data collected at 7 TeV were reported in Ref. [40], where a lower limit of 2.21 TeV on the mass of the sequential standard model (SSM) Z' boson is set, rescalable to 1.78 TeV in the case of a Z'_N boson. Limits were also reported by CMS in Ref. [41] for 1.1 fb^{-1} of luminosity but have now been superseded by one at full luminosity [42] which has just been announced as this paper is finalized, setting a lower limit of 2.08 TeV on the mass of the Z'_N boson.

However the limits quoted by ATLAS and CMS are for the specified Z' couplings with the assumption that the decay into SM particles provides the only kinematically allowed decay channels. In Ref. [15] the impact of exotics' decay width was studied and a considerable impact was found for two test case benchmarks. Based on the work in Ref. [43] we then used the branching ratios for those benchmarks (which reduced the branching into leptons, compared to ignoring exotic decays, by about a factor of 2) to rescale the cross section prediction, and we obtained an estimate of how the limit can change when light exotics, if present, are taken into account. For example if we assume a similar impact from exotics (i.e., a dilution of the leptonic branching ratio by a factor of 2) then the limit on the Z'_N mass could be reduced from 2.02 TeV to somewhere around 1.8 TeV, as can be seen from examining Fig. 6 of Ref. [42].

However one should note that not only is this a fairly simple estimate, it is also dependent on the details of the spectrum and the masses of the various exotic states. However the first two generations of singlinos had a significant contribution to the width and light singlinos are always present; therefore the limit will always be significantly smaller than that quoted by assuming no available exotic decay channels.

The benchmarks and plots presented here all have a Z' mass above 1.8 TeV and in all but one plot and benchmark (where $M_{Z'} = 1.889 \text{ TeV}$) also above the quoted limit, assuming no exotics, and therefore clearly safe in this respect.

IV. DARK MATTER CONSTRAINTS

We now consider the question of cosmological cold dark matter (CDM) relic abundance due to the neutralino LSP. In the considered benchmark points we have a predominantly binolike lightest neutralino with a mass $|m_{\chi_1^0}|$. One might be concerned that such a bino might give too large a contribution to Ω_{CDM} . Indeed a recent calculation of Ω_{CDM} in the USSM [44], which includes the effect of the MSSM states plus the extra Z' and the active singlet S , together with their superpartners, indicates that for the benchmarks considered here that Ω_{CDM} would be too large. However the USSM does not include the effect of the extra inert Higgs and Higgsinos that are present in the E_6 SSM, and so we need to discuss their effect on the relic density.

In our analysis we have considered the inert Higgsino masses given by $\mu_{\tilde{H}}(\alpha) = \lambda_\alpha s / \sqrt{2}$. We have not considered the mass of the inert singlinos. In general, these are generated by mixing with the Higgs and inert Higgsinos, and are thus of order $f v^2 / s$, where f are additional Yukawa couplings that we have not specified in our analysis. Since $s \gg v$ it is quite likely that the LSP neutralino in the eE_6 SSM will be an inert singlino with a mass lighter than 60 GeV. This would imply that the state χ_1^0 considered here is not cosmologically stable but would decay into lighter states consisting of admixtures of inert singlinos and inert Higgsinos. Such states can annihilate via an s -channel Z boson, due to their doublet component, yielding an acceptable CDM relic abundance, as has been recently demonstrated in the E_6 SSM [45]. However, in such a scenario, the lightest inert neutralino states would have sizable couplings to the Higgs boson, leading to significant modifications of Higgs phenomenology, and a contribution to the direct detection cross section due to Higgs exchange which conflicts with the XENON-100 limit in the region of parameter space where the correct relic abundance is achieved [46]. There are several ways out of this problem, as discussed in Ref. [47]. For example, the light inert states may have masses around the keV and GeV energy scale, evading the XENON-100 search limits, and leading to warm dark matter [48]. Many of these possibilities lead to novel gluino decays into the extra lighter neutralinos and charginos, which can modify significantly the gluino search limits and strategies as discussed in Ref. [47].

In this paper we shall consider the approach to CDM in the E_6 SSM proposed in Ref. [19]. The idea is to set the inert singlino $\tilde{S}_{1,2}$ couplings f to zero so that they are exactly massless, with their couplings forbidden by a discrete symmetry. The massless $\tilde{S}_{1,2}$ singlinos will contribute to the effective number of neutrino species in the early Universe giving $N_{\text{eff}} \approx 3.2$, but will otherwise be unobservable, except in Z' decays. In particular they play no part in dark matter. Thus, the binolike state with a mass $|m_{\chi_1^0}|$ will be cosmologically stable and will be a CDM candidate. In order to achieve the observed WMAP relic

abundance, we shall tune the mass of the lightest inert Higgsino mass $\mu_{\tilde{H}}(1) = \lambda_1 s / \sqrt{2}$ to be just above the bino mass. The idea is that the bino up-scatters into the nearby inert Higgsinos which subsequently efficiently annihilate via a Z boson into SM particles [19]. Note that the inert Higgsinos have full electroweak strength couplings to the Z boson. In practice the correct relic abundance can be achieved by tuning the inert Higgsinos to be about 10 GeV heavier than the bino [19],

$$\mu_{\tilde{H}}(1) \approx |m_{\chi_1^0}| + 10 \text{ GeV}. \quad (10)$$

In the parameter space scans discussed later we do not directly impose this condition, since we do not know the bino mass at the outset. However it is always possible to satisfy Eq. (10) by tuning $\lambda_1(M_X)$, the Yukawa coupling which fixes the lightest inert Higgsino mass. Additionally $\lambda_2(M_X)$ (Yukawa coupling for the heaviest inert Higgsino) can be tuned to compensate the impact on the RGEs such that the rest of the mass spectrum is unchanged. Therefore Eq. (10) can be satisfied for every point on all of the plots shown. All benchmarks presented will also be required to satisfy this condition.

We emphasize that, in this scenario, the gluino decays will be just those of the MSSM with a binolike LSP, so standard MSSM gluino searches and limits will also apply to the E_6 SSM.

V. RESULTS

A. Exploration of the parameter space

The LHC limits coming from searches for a Z' , squarks and gluinos, and the Higgs restrict the parameter space of the model in complementary ways. Additionally the tentative signal Higgs signal between 124–126 GeV, if confirmed and the mass precisely measured, would also substantially improve our knowledge of the cE_6 SSM parameters. One should also note that as described in Refs. [10,11] studies based on the (unconstrained) E_6 SSM showed that the light Higgs can be substantially heavier in the E_6 SSM than in the MSSM so there is significant reason for optimism that this signal could be comfortably accommodated in this model.

To explore this further we carried out a number of scans over the parameter space. In each scan we fixed s (and therefore the Z' mass) so that the Z' mass is above the experimental limit. For scenarios where the Z' is below its mass limits, most of the parameter space would also have gluinos below the limit suggested by the LHC searches. However the gluino limit still plays an important role in restricting the allowed parameter space for higher values of s . The allowed masses of the Higgs and the tentative signal seem to be more compatible with a heavier Z' , and also provide information about the cE_6 SSM parameters even well above the limits from gluinos/squarks and Z' .

1. Spectrum generator

The cE_6 SSM mass spectrum is calculated from the input parameters using a spectrum generator first written for [13] where the procedure is described in detail. However here we summarize the procedure for the purposes of completeness. The fundamental parameters of the cE_6 SSM are a unified gauge coupling, Yukawa couplings of the observed fermions, new exotic Yukawa couplings λ_i and κ_i (where $i = 1\dots 3$) and universal soft masses m_0 , $M_{1/2}$ and A . The gauge and Yukawa couplings and the combination of VEVs $v^2 = v_1^2 + v_2^2$ are constrained by experiment at low energies.

To find solutions consistent with both the high scale universality constraints and this low energy data, we evolve between the high and low scales with RGEs² and impose EWSB conditions by finding simultaneous solutions to the three quadratic minimization equations which at tree level are functions of $\{m_0, M_{1/2}, A, s, v_u, v_d, \lambda(Q), g, g', g'_1\}$. Since g and g' are fixed by experiment and g'_1 is then fixed from requiring gauge coupling unification of all four gauge couplings the three constraints mean that we must have three of $\{m_0, M_{1/2}, A, s, \tan\beta, \lambda(Q)\}$ as outputs to fix $M_Z = 91.1876$ GeV, and we chose m_0 , $M_{1/2}$ and A since the values of $\tan\beta$ and $\lambda(Q)$ are required at the very outset of the calculation to perform the SUSY renormalisation group (RG) evolution.

Since the three quadratic equations correspond to one quartic equation we have four solutions for the soft masses for each set of input parameters, so our procedure yields between zero and four real solutions for each point. Finally leading one-loop contributions to the effective potential are then included iteratively and the spectrum is then determined.

Therefore our input parameters are $\{\lambda_i(M_X), \kappa_i(M_X), s, \tan\beta\}$. Since we are interested in constraints coming from squarks and gluinos in the parameter space scans we fix $\kappa_{1,2,3} = \kappa$ to keep the colored exotics heavy, but since the inert Higgsinos and inert Higgs are only weakly produced we left $\lambda_{1,2} = 0.1$, which is consistent with the previous study of the parameter space where we focused on lighter scenarios [13]. So here we investigate a subspace of the full model where we have only four free parameters $\lambda = \lambda_3, \kappa, \tan\beta, s$.

Having the soft masses as output parameters makes finding iterative solutions, including leading tadpole terms, trickier than in the MSSM where $\tan\beta$ and M_Z can be traded for μ and $B\mu$. Without knowing the soft masses at the outset the stop masses cannot be estimated initially, and starting without the leading one-loop contributions in the EWSB iteration can lead to a significant border region in the parameter space where an EWSB condition can be

²As already described in Sec. II, we used two-loop RGEs for gauge couplings, Yukawa couplings, gaugino masses and trilinear soft couplings and one-loop RGEs for scalar masses.

found for the one-loop effective potential but missed in the tree-level approximation.

To resolve this we perform the parameter space scans over a fine grid (rather than employing more sophisticated random sampling scans) and use the solution from the previous step as an initial guess for the tadpoles in the next step. This approach leads to $m_0 - M_{1/2}$ plots where the density of the points varies so some regions are very densely populated, while others are sparsely populated. In addition the lower stability of a routine outputting soft masses from the EWSB conditions and the fact that we have a multiplicity of solutions for the soft masses (leading to folds in the parameter space where obtaining a solution can be dependent on the direction one moves through it) renders the search for solutions a nontrivial task even with a fine grid scan. Due to these issues we also cannot guarantee that we find all potential solutions; however it is clear that certain regions must be excluded for reasons stated in the subsequent text.

The spectrum is then calculated using the expressions presented in Ref. [13]. The most important constraints come from the gluino and the Higgs, so we include one-loop shifts to pole for gluino mass and leading two-loop corrections for the lightest Higgs mass.

2. Higgs and gluino contours

In each plot we fix s and $\tan\beta$ then vary λ between -3 and 0 (thus fixing $\mu_{\text{eff}} < 0$) and κ between 0 and 3 . The restriction to $\mu_{\text{eff}} < 0$ is to remove a confusing bifurcation in the gluino contours at large m_0 .

First in light of the exciting progress and effectiveness of the LHC in probing scenarios with multiple TeV scenarios we update Fig. 4 from Ref. [13] to show the full range of $m_0 - M_{1/2}$ rather than cutting off at around a TeV, and we also show even very heavy values of s which are not immune to LHC searches and will certainly be probed by a Higgs mass measurement. In Fig. 1 we plot the allowed values of $m_0 - M_{1/2}$ for all the solutions we find for $\tan\beta = 10$ and fixed values of $s = 5, 10, 20, 50, 100$ TeV. Since here we are going to use the plots to help us estimate the LHC constraints in the $cE_6\text{SSM}$ and also to match the plot we are updating, we impose only constraints prior to the LHC, which are specified in Ref. [13]. Also note in order to match more closely results published by the experimental analyses (where they interpret the search constraints in terms of the $c\text{MSSM}$) we have switched the x and y axes so that $M_{1/2}$ now appears on the y axis and m_0 on the x axis.

Notice that while increasing s pushes up the lower limit on m_0 (below this the inert Higgs run below their LEP limit and rapidly become tachyonic), and the upper limit on $M_{1/2}$ (above which no solution satisfying both EWSB and universality conditions can be found) also increases, low $M_{1/2}$ is always possible and is only bounded by the constraints from gauginos (the update of which we will discuss shortly). Therefore squark/gluino searches can

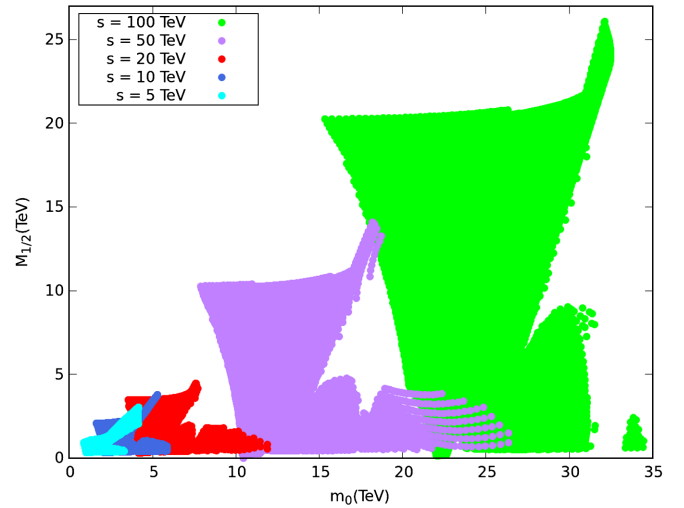


FIG. 1 (color online). Allowed region for $cE_6\text{SSM}$ with $\tan\beta = 10$, $s = 5, 10, 20, 50, 100$ TeV in cyan (light grey), blue (medium-dark grey), red (dark grey), purple (medium-light grey) and green (medium grey) respectively with $\lambda_{12} = 0.1$, while contours are produced with a universal κ coupling and λ_3 are varied, with λ_3 (and hence $\mu_{\text{eff}} \leq 0$).

always impact part of the parameter space for any value of s , albeit an increasing small fraction of the total parameter space as we go up in s .

Note also that in addition to some regions being sparsely populated, the reasons for which are explained above, we also see a significant gap in the plot of allowed solutions for each value of s . Interestingly the solutions for $\mu_{\text{eff}} > 0$ (not shown here) although covering a substantially smaller region of the parameter space do tend to cover these gap regions.

Now we want to understand how the squark/gluino searches and Higgs limits constrain the parameter space and where (or if) we can fit the tentative Higgs signal.

In Fig. 2, the squark and gluino contours are shown (left) beside the Higgs masses (right) for $\tan\beta = 10$, $s = 5$ TeV. The squark contours are specifically of the left handed squark mass for the first two generations (it is contours of this squark mass which were plotted on the ATLAS and CMS papers). Both those and the gluino contours are formed by selecting points from the scans where the mass lies in a suitably narrow range such that the width of the contour gives a resolvable line for the scale of the plot.

For any given gluino mass we find that squark masses must be substantially heavy. For example if we take the latest limits on the gluino coming from the LHC which apply in the large m_0 region, which is about 840 GeV as described in Sec. III B, then we find no solutions with squarks below 1.8 TeV, rendering the larger limits found for the $c\text{MSSM}$ (see Fig. 7(a) of Ref. [27]) in the low m_0 region irrelevant. Therefore we conclude that the squark and gluino constraints place a limit on $M_{1/2}$ at around 1 TeV.

The right plot showing Higgs masses gives a very different picture. The Higgs mass varies over the plane (driven to

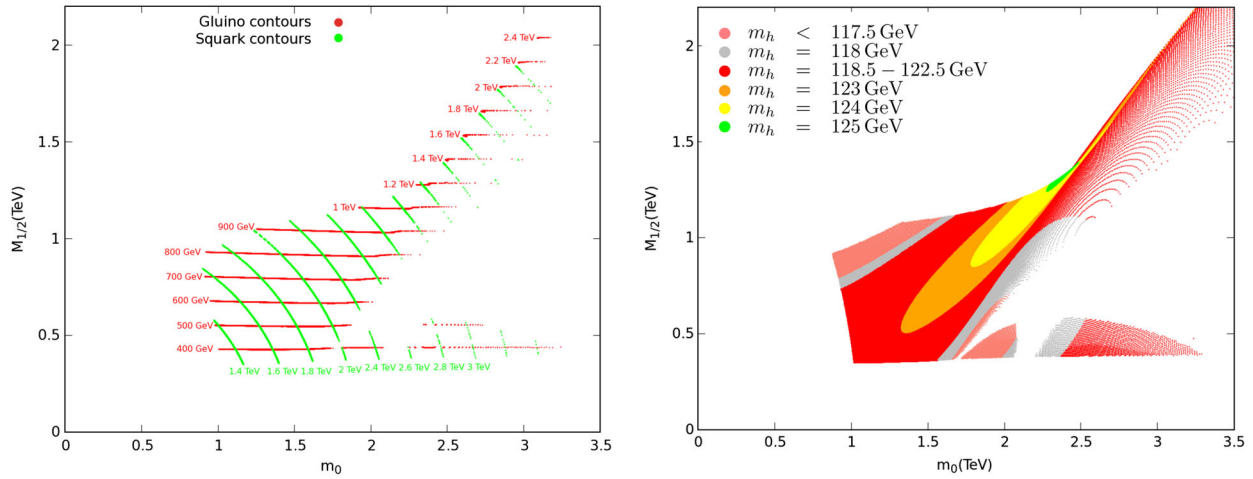


FIG. 2 (color online). Squark and gluino mass contours (left panel) and Higgs mass contours (right panel) in the $(m_0, M_{1/2})$ plane of the cE6SSM with $\tan\beta = 10$, $\lambda_{12} = 0.1$, $s = 5$ TeV, corresponding to $M_{Z'} = 1.889$ TeV. Scans are produced with a universal κ coupling varied over $\{0, 3\}$ and λ_3 over $\{-3, 0\}$ respectively so that $\mu_{\text{eff}} \leq 0$.

a substantial degree by the variation of λ) in a very non-trivial manner. Different values of the Higgs mass are plotted where the values quoted in the key are the central values in bin with a ± 0.5 GeV width. Remarkably the Higgs mass varies over the plane within a very narrow set of values that include the mass of the tentative signal.

A substantial region of the parameter space is ruled out by having m_h in the range 118.5–122.5 GeV (red) and $m_h < 117.5$ GeV (pink). However, in addition to the 118 GeV (gray) gap in the lower mass exclusion, there is still a significant region towards the center of the plot which is allowed and even where the tentative signal can be matched. This is mainly for Higgs masses of 124 GeV, as 125 GeV only gives a small region and a 126 GeV Higgs cannot be realized for these choices of s and $\tan\beta$. If we also take into

account the new LHC gluino constraints one can see that little of the 124 GeV signal is affected while most of the available space for a 123 GeV Higgs is removed.

However there are still strong constraints on the parameter space coming from the Higgs limits alone, and it is clear one must be careful to apply both of these complimentary constraints in order to understand where the viable regions are.

So while $s = 5$ TeV has a substantial portion of allowed parameter region which can accommodate the tentative Higgs signal, a measurement of the Higgs mass of 126 GeV could potentially rule this out. Therefore it is important to consider other slices of our four dimensional parameter space.

In Fig. 3 we increase s to 10 TeV, but keep $\tan\beta = 10$ and from the left plot we can see that again the squark

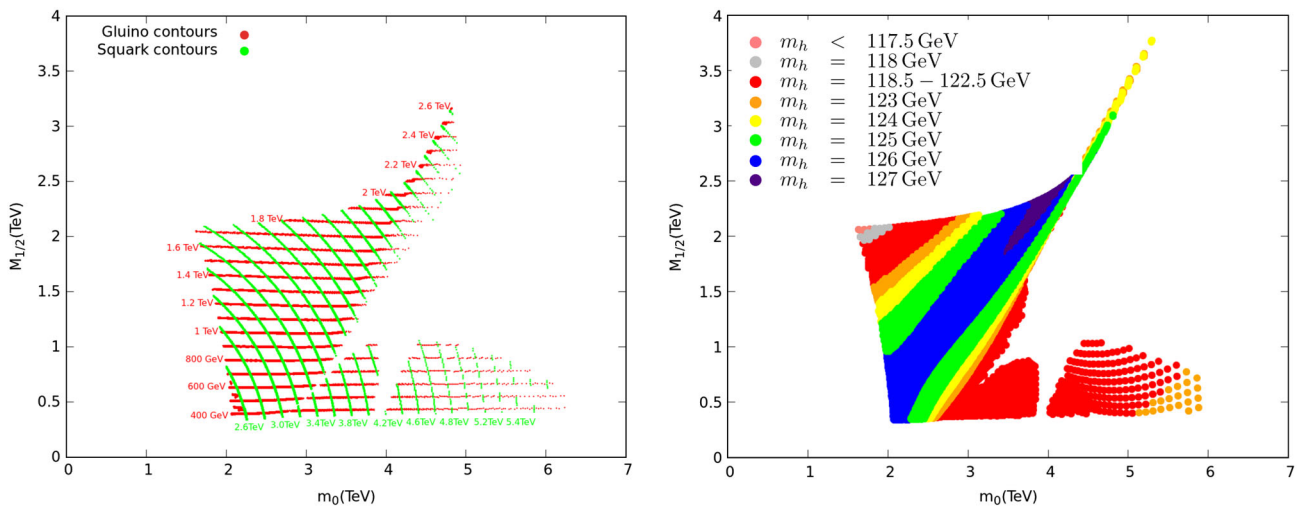


FIG. 3 (color online). Squark and gluino mass contours (left panel) and Higgs mass contours (right panel) in the $(m_0, M_{1/2})$ plane of the cE6SSM with $\tan\beta = 10$, $\lambda_{12} = 0.1$, $s = 10$ TeV, corresponding to $M_{Z'} = 3.778$ TeV. Scans are produced with a universal κ coupling varied over $\{0, 3\}$ and λ_3 over $\{-3, 0\}$ so that $\mu_{\text{eff}} \leq 0$.

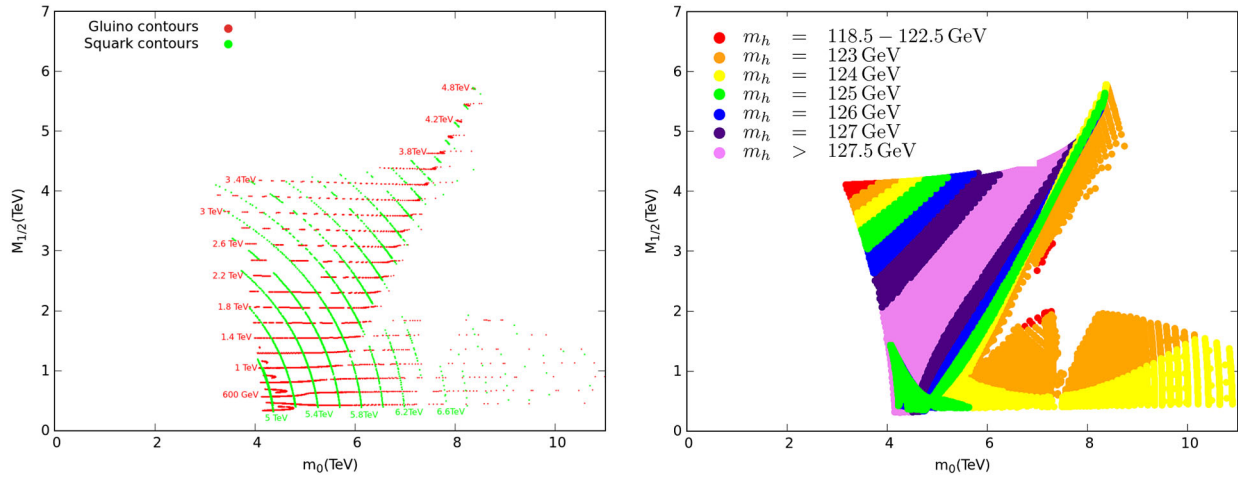


FIG. 4 (color online). Squark and gluino mass contours (left panel) and Higgs mass contours (right panel) in the $(m_0, M_{1/2})$ plane of the cE6SSM with $\tan\beta = 10$, $\lambda_{12} = 0.1$, $s = 20$ TeV, corresponding to $M_{Z'} = 7.564$ TeV. Scans are produced with a universal κ coupling varied over $\{0, 3\}$ and λ_3 over $\{-3, 0\}$ so that $\mu_{\text{eff}} \leq 0$.

and gluino search constraints can all be satisfied by a simple cut on $M_{1/2}$ at 1 TeV, but now there is a substantially greater proportion of the parameter space which is above this limit since the upper limit on $M_{1/2}$ is increasing with s . Additionally, in the right plot, we also see that all masses of the tentative Higgs signal region can be comfortably accommodated and this region fills most of the allowed parameter space that is above the $M_{1/2} > 1$ TeV limit we have set from squark and gluino searches.

In Fig. 4 we see that if we increase the singlet VEV further to $s = 20$ TeV then we are no longer restricted by the lower limits on the Higgs mass, with only a few points having a Higgs mass of 122 GeV, but now there is a substantial region ruled out by the upper limit $m_h \geq 127.5$ set by CMS.

Figures 5 and 6 demonstrate that even with very heavy s values, such that the Z' is well beyond reach of the LHC, not only is there still a small region of parameter space where the gluino is observable, but additionally a Higgs mass measurement would yield useful information about the parameter space well above what can actually be constrained from direct searches. This illustrates the significance of the Higgs to providing constraints and measurement of cE₆SSM parameters.

Notice also that while in much of the parameter space new physics states are out of reach, reducing the $\lambda_{1,2}$ coupling such that the inert Higgsinos are observable would not perturb the RG evolution much, so these plots remain a very good approximation. Thus they reveal an interesting potential scenario where only the inert Higgsinos and the SM-like Higgs are discovered, but an

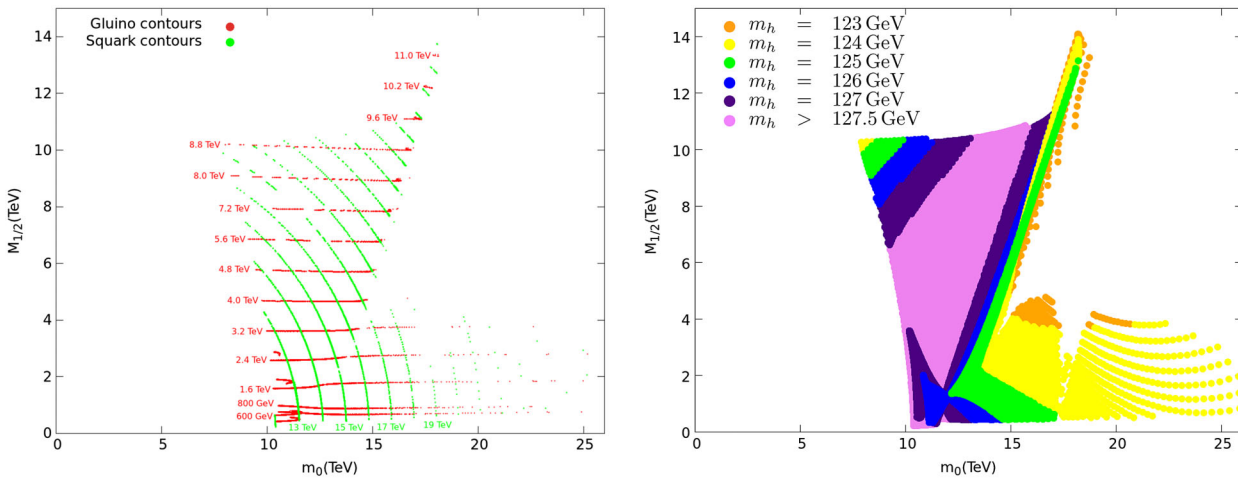


FIG. 5 (color online). Squark and gluino mass contours (left panel) and Higgs mass contours (right panel) in the $(m_0, M_{1/2})$ plane of the cE6SSM with $\tan\beta = 10$, $\lambda_{12} = 0.1$, $s = 50$ TeV, corresponding to $M_{Z'} = 18.996$ TeV. Scans are produced with a universal κ coupling varied over $\{0, 3\}$ and λ_3 over $\{-3, 0\}$ so that $\mu_{\text{eff}} \leq 0$.

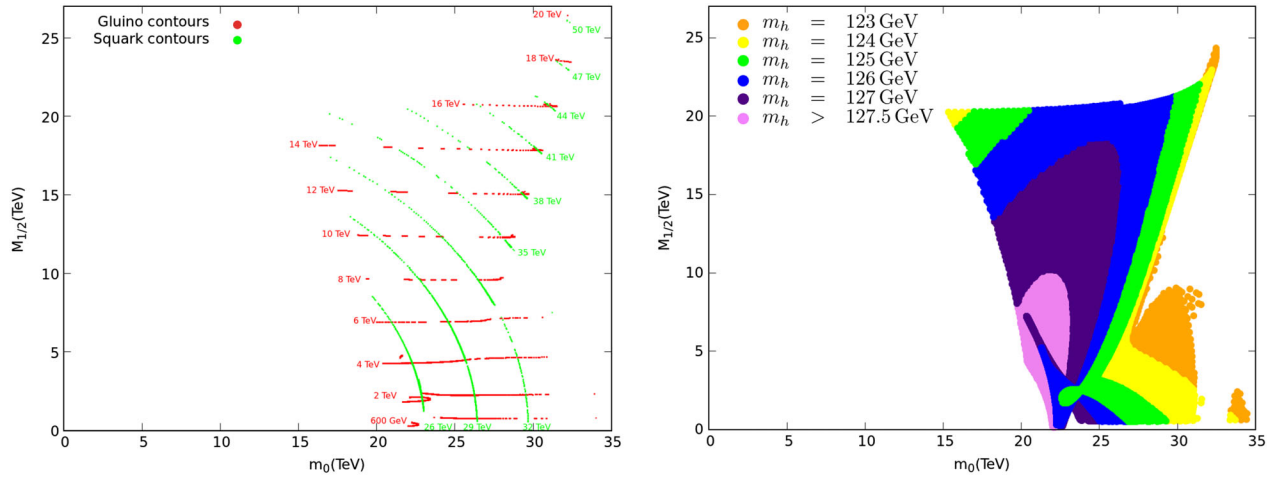


FIG. 6 (color online). Squark and gluino mass contours (left panel) and Higgs mass contours (right panel) in the $(m_0, M_{1/2})$ plane of the cE6SSM with $\tan\beta = 10$, $\lambda_{12} = 0.1$, $s = 100$ TeV, corresponding to $M_{Z'} = 37.808$ TeV. Scans are produced with a universal κ coupling varied over $\{0, 3\}$ and λ_3 over $\{-3, 0\}$ so that $\mu_{\text{eff}} \leq 0$.

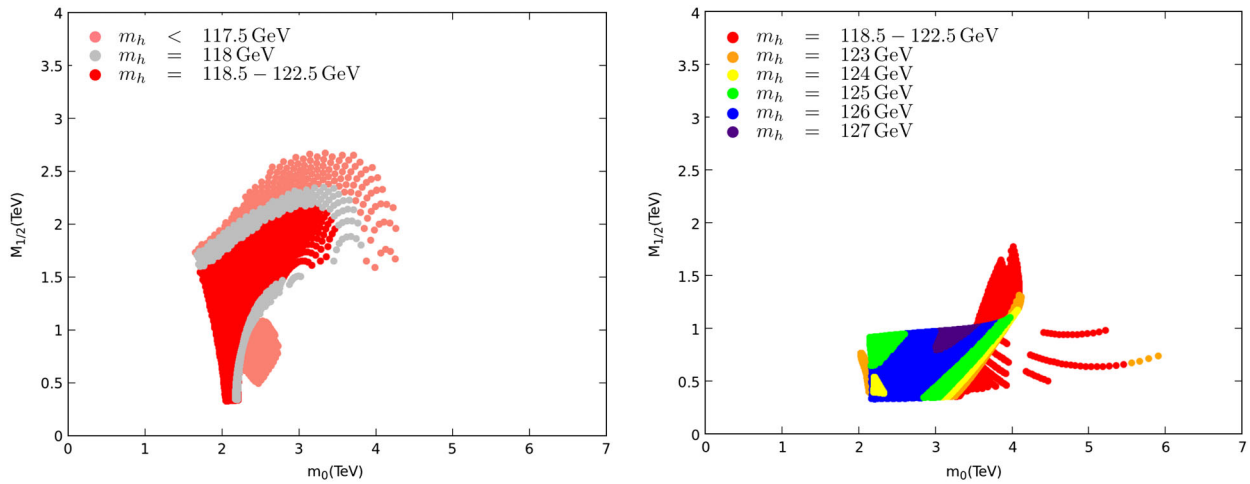


FIG. 7 (color online). Higgs mass contours for $\tan\beta = 3$ (left panel) and $\tan\beta = 30$ (right panel) in the $(m_0, M_{1/2})$ plane of the cE6SSM with $\lambda_{12} = 0.1$, $s = 10$ TeV, corresponding to $M_{Z'} = 3.779$ TeV. Scans are produced with a universal κ coupling varied over $\{0, 3\}$ and λ_3 over $\{-3, 0\}$ so that $\mu_{\text{eff}} \leq 0$.

accurate Higgs mass measurement would give a great deal of information on the parameter space.

Finally we comment on the $\tan\beta$ dependence of these results. The form of the squark and gluino contours is not substantially modified by changing $\tan\beta$ so we do not reproduce these plots here. However the allowed region of parameter space is dramatically changed, as are the Higgs masses. This is illustrated in Fig. 7 where we plot the allowed region of the parameter space for $s = 10$ TeV and $\tan\beta = 3$ (left) and $\tan\beta = 30$ (right). Here we see that the combination $s = 10$ TeV and $\tan\beta = 3$ is almost entirely ruled out with only the 118 GeV window left. On the other hand for $\tan\beta = 30$ most of the parameter space is compatible with the tentative Higgs signal and, in particular, a Higgs of 126 GeV appears very typical.

However the overall allowed region of the parameter space has significantly shrunk in comparison to the $\tan\beta = 10$ case.

B. Benchmark points

We have chosen five benchmark points that reproduce a Higgs mass of around 125 GeV, in order to demonstrate significant and interesting features that may arise in the cE6SSM. These benchmarks are given in Table II, labeled HBM1 to HBM5 (for heavy benchmark). All of these benchmarks evade current experimental constraints, but predict new particle states that may be found at the LHC. They represent a wide selection of different scales for the scalar VEV, with s ranging from 5 TeV up to 100 TeV. As

TABLE II. Parameters and masses for the new heavier benchmarks with Higgs masses in the range of the tentative signal at $m_h = 124\text{--}125$ GeV.

	HBM1	HBM2	HBM3	HBM4	HBM5
$\tan\beta$	10	10	10	10	10
$\lambda_3(M_X)$	-0.22	-0.35	-0.55	-0.15	-0.16799
$\lambda_2(M_X)$	0.1373	0.141	0.035	0.12	0.1427
$\lambda_1(M_X)$	0.0374	0.0299	0.0252	0.006	0.00237
$\kappa_3(M_X)$	0.17	0.45	0.9	0.9	0.3655
$\kappa_{1,2}(M_X)$	0.17	0.02	0.02	0.015	0.3655
s [TeV]	5	10	20	50	100
$M_{1/2}$ [GeV]	1135	1570	1847	1259	1148
m_0 [GeV]	2158	2490	4698	16106	27109
A_0 [GeV]	-266	2010	8759	-1658	-24825
$m_{\tilde{D}_1}(3)$ [GeV]	2403	5734	14343	39783	48516
$m_{\tilde{D}_2}(3)$ [GeV]	3315	7961	16658	40838	53511
$\mu_D(3)$ [GeV]	1748	6725	15570	39925	48820
$m_{\tilde{D}_1}(1, 2)$ [GeV]	2403	2366	3141	12435	48516
$m_{\tilde{D}_2}(1, 2)$ [GeV]	3314	2899	4268	13869	53511
$\mu_D(1, 2)$ [GeV]	1748	368	521	1025	48820
$ m_{\chi_6^0} $ [GeV]	1982	3908	7722	1900	37877
$m_{h_3} \simeq M_{Z'}$ [GeV]	1889	3779	7564	18996	37808
$ m_{\chi_5^0} $ [GeV]	1802	3655	7410	18822	37740
$m_S(1, 2)$ [GeV]	2567	3680	7148	20937	38076
$m_{H_2}(2)$ [GeV]	2163	2463	3491	14680	24028
$m_{H_1}(2)$ [GeV]	2084	1834	2440	12151	18575
$m_{H_2}(1)$ [GeV]	2092	2060	3460	13728	21200
$m_{H_1}(1)$ [GeV]	2015	1670	2452	12355	17507
$\mu_{\tilde{H}}(2)$ [GeV]	680	1120	427	3813	9967
$\mu_{\tilde{H}}(1)$ [GeV]	187	257	307	192	167
$m_{\tilde{u}_1}(1, 2)$ [GeV]	2689	3450	5818	17254	29663
$m_{\tilde{u}_2} \simeq m_{\tilde{d}_1}(1, 2)$ [GeV]	2743	3531	5885	17264	29668
$m_{\tilde{d}_2}(1, 2)$ [GeV]	2749	3644	6285	18260	31981
$m_{\tilde{e}_1}(1, 2, 3)$ [GeV]	2272	2815	5310	17190	29631
$m_{\tilde{e}_2}(1, 2, 3)$ [GeV]	2405	3139	5884	18204	31956
$m_{\tilde{\tau}_1}$ [GeV]	2254	2788	5230	17020	29373
$m_{\tilde{\tau}_2}$ [GeV]	2396	3127	5849	18127	31837
$m_{\tilde{\nu}_2}$ [GeV]	2729	3510	6201	18123	31767
$m_{\tilde{\nu}_1}$ [GeV]	2370	2979	4621	14632	25421
$m_{\tilde{\nu}_2}$ [GeV]	2381	2994	4634	14633	25422
$m_{\tilde{\nu}_1}$ [GeV]	1877	2220	2877	11607	20632
$ m_{\chi_{3,4}^0} \simeq m_{\chi_2^\pm} $ [GeV]	867	2281	4897	3819	9398
$m_{h_2} \simeq m_A \simeq m_{H^\pm}$ [GeV]	1890	2742	5254	5254	19474
m_{h_1} [GeV]	124	124	124	125	125
$m_{\tilde{g}}$ [GeV]	984	1352	1659	1129	1001
$ m_{\chi_4^\pm} \simeq m_{\chi_3^0} $ [GeV]	313	439	526	324	280
$ m_{\chi_1^0} $ [GeV]	177	247	297	182	157

discussed in the last section, low $\tan\beta$ has difficulty reproducing a 125 GeV Higgs boson, while high $\tan\beta$ suffers from a restricted parameter space due to the requirements of correct EWSB, so for all these benchmarks we adopt a medium value of $\tan\beta = 10$. All benchmarks have a reasonably low value for the mass of the lightest neutralino, which is a consequence of choosing reasonably low values of $M_{1/2}$ thereby ensuring a small bino mass within reach of

the LHC (in these scenarios, the lightest neutralino is always predominantly a bino). This also means that the gluino stays reasonably light in all these scenarios too (though still above current LHC exclusion). Furthermore, all five benchmarks conform to the condition of Eq. (10) where the lightest inert Higgsino is 10 GeV heavier than the lightest neutralino, thereby giving a correct dark matter relic abundance, as discussed in Sec. IV

HBM1 is an example benchmark with $s = 5$ TeV and a Higgs mass of 124 GeV. We have lifted the previous degeneracy $\lambda_1 = \lambda_2$ used in our scans over the parameter space, in order to ensure that Eq. (10) is satisfied. However, since varying λ_2 will only affect the mass of the inert Higgs and Higgsinos, this can be done for any point that we found in our scans, yielding an identical spectrum except for the inerts. Consequently, HBM1 may be thought of as one of the points seen in the yellow region of Fig. 2. Since this is our benchmark with the lowest value of s , it also contains the lightest Z' with a mass of 1889 GeV, just a little beyond current LHC bounds and possibly detectable reasonably soon. The rather small value of m_0 results in reasonably light squarks and sleptons that would be observable at the LHC once more luminosity is gathered. Finally, since $\kappa_1 = \kappa_2 = \kappa_3$, the scalars \tilde{D}_1 and \tilde{D}_2 are separately degenerate over the three generations, and are light enough to be produced at the LHC. Recall that these scalars are even under the analogue of R parity, so may be produced singly and need not decay to the LSP.

For HBM2 we increase s up to 10 TeV, but many of the features of HBM1 remain unchanged. Again, we have a Higgs boson mass of 124 GeV, a light neutralino, with accompanying inert Higgsino to provide the correct dark matter abundance, and relatively light squarks, sleptons and gluino. However, for this benchmark we lift the degeneracy in $\kappa_{1,2,3}$ and allow $\kappa_{1,2}$ to be considerably smaller than κ_3 . This scenario therefore cannot be directly matched to one of the points in our scan of Fig. 3. Choosing small $\kappa_{1,2}$ pushes down the mass of the exotic D quarks to 368 GeV, allowing them to be pair produced at the LHC via their QCD coupling. For a detailed discussion of this exotic quark production, see Ref. [15], where benchmark C contains exotic quarks with a very similar mass.

One may be concerned that such a light mass for an exotic quark is ruled out by the LHC; however as described in Sec. III C the constraints which have so far been presented are not directly applicable to this case and the detailed studies required to determine limits on our exotic quarks have not yet been carried out. These benchmarks are intended to motivate and aid precisely these urgently needed investigations. Additionally since we obtain the light exotic quarks by setting the $\kappa_{1,2}$ couplings to be very small, these can be adjusted to raise the mass of the exotic quarks to 1 TeV (corresponds to $\kappa_{1,2} \approx 0.055$) without changing the rest of the spectrum by more than $\approx 10\%$.

We keep these exotic D quarks relatively light also in HBM3, by keeping the same low value of $\kappa_{1,2}$. This scenario has a scalar VEV with $s = 20$ TeV, and one can see that the third generation exotic D quarks, whose mass is fed by a rather large value of κ_3 , become very heavy—over 15 TeV. In HBM4 our scalar VEV becomes very large indeed, with $s = 50$ TeV, but maintains reasonably light first and second generation exotic D quarks, now with 1025 GeV, which should still be within reach of the LHC. This is despite

now having a large value for m_0 , and consequently squarks that are way beyond the reach of the LHC.

Finally, we give an example of a benchmark, HBM5, where most of the states are extremely heavy, with $s = 100$ TeV. Here, we only make two concessions towards a light spectrum: firstly, we keep $M_{1/2}$ small, which keeps our two lightest neutralinos and our lightest chargino light, and our gluino relatively light; and secondly, we maintain a small value of λ_1 to provide a light inert Higgsino that can satisfy Eq. (10). In this scenario we have returned to degenerate κ_i , so this example is one of the green points in Fig. 6. Without the small value of $\kappa_{1,2}$, the exotic D quarks become extremely heavy (of order 50 TeV) well beyond the search reach of the LHC. However, even for supersymmetric scenarios with $s = 100$ TeV we may still have new supersymmetric particles to be discovered at the LHC, since the gaugino sector and a few inert Higgs states are still accessible.

Further studies on these benchmarks will be facilitated by the implementation of the E_6 SSM into codes like SARAH [49] and CALCHEP [50], which are in preparation [51] and also an extension of tools developed for Ref. [47] to include all exotic states in the E_6 SSM.

VI. CONCLUSIONS

In this paper we have studied the parameter space of the constrained exceptional supersymmetric standard model (cE_6 SSM) consistent with a Higgs signal near 125 GeV and the LHC searches for squarks, gluinos and Z' . The cE_6 SSM parameter space, consistent with correct electro-weak symmetry breaking, is represented by scans in the $(m_0, M_{1/2})$ plane for fixed Z' mass and $\tan\beta$, with squark, gluino and Higgs masses plotted as contours in this plane. Although the heaviest Higgs masses are achievable for the largest values of λ , EWSB is achieved in the cE_6 SSM for smaller values of λ . This is because EWSB requires reasonably large values of κ_i which drive m_S^2 negative, and such values of κ_i restrict the values of λ that can be achieved consistent with these couplings remaining perturbative. This means that in practice, the tree-level contribution to the Higgs mass in the cE_6 SSM is only slightly larger than in the MSSM, so that a 125 GeV Higgs mass requires a very large loop contribution, similar to the case of the MSSM. For this reason we have focused on values of $\tan\beta = 10$, avoiding the very large values of $\tan\beta$ that may raise other phenomenological issues arising from processes such as $B_s \rightarrow \mu\mu$.

We find that a 125 GeV Higgs mass only arises for a sufficiently large Z' mass, mainly above current limits. To be precise, the value of $s = 5$ TeV corresponding to $M_{Z'} \sim 2$ TeV only has a very small region of parameter space consistent with a 125 GeV Higgs boson, although there is a larger region available for 124 GeV or lighter Higgs bosons. As expected, heavier Higgs bosons are more easily achieved over large regions of parameter space for larger

values of $s = 10\text{--}100\text{TeV}$. For each of these cases there are two distinct regions of the $(m_0, M_{1/2})$ plane consistent with a 125 GeV Higgs boson, where both regions correspond to multi-TeV squark masses, but with one of the regions always extending down to relatively light gluinos, winos and binos, where the gluinos are typically within reach of the LHC in the 8 TeV or forthcoming 14 TeV runs. Successful dark matter relic abundance may be achieved over all the parameter space, assuming a binolike LSP with a nearby heavier inert Higgsino doublet, about 10 GeV heavier, and decoupled inert singlinos. This scenario will therefore result in conventional gluino decay signatures similar to those of the MSSM in the region of parameter space with lighter gluinos and very heavy squarks and sleptons. This is similar to the focus point of the MSSM, but with the relic abundance here resulting from the nearby inert Higgsinos (about 10 GeV heavier than the bino) which provide the distinguishing phenomenological prediction of the $cE_6\text{SSM}$ in this scenario.

A set of benchmark points with a Higgs near 125 GeV has been provided which exemplifies the above features and in addition highlights other features of phenomenological interest such as exotic D fermions within reach of

the LHC. All these benchmarks also exhibit gluinos, winos and binos and inert Higgsinos, within reach of the forthcoming runs of the LHC, providing the exciting possibility of SUSY discovery even for squarks and sleptons outside the range of the LHC. These results show that there is still a vast parameter space of the $cE_6\text{SSM}$ to be explored, with heavier squarks and sleptons and lighter gauginos remaining a firm prediction of the model.

ACKNOWLEDGMENTS

SFK acknowledges partial support from the STFC Consolidated ST/J000396/1 and EU ITN Grants No. UNILHC 237920 and INVISIBLES 289442. SM is partially supported through the NExT Institute. DJM acknowledges partial support from the STFC Consolidated Grant No. ST/G00059X/1. The work of RN was supported by the U.S. Department of Energy under Contract No. DE-FG02-04ER41291. The work of PA is supported by the ARC Centre of Excellence for Particle Physics at the Terascale. PA would like to thank M. Schönerr, D. Stöckinger and Tony Williams for helpful comments and discussions regarding this work.

-
- [1] G. Aad *et al.* (ATLAS Collaboration), *Phys. Lett. B* **710**, 49 (2012).
- [2] S. Chatrchyan *et al.* (CMS Collaboration), *Phys. Lett. B* **710**, 26 (2012).
- [3] G. Kane, P. Kumar, R. Lu, and B. Zheng, *Phys. Rev. D* **85**, 075026 (2012); I. Gogoladze, Q. Shafi, and C. S. Un, *J. High Energy Phys.* **08** (2012) 028; A. Arbey, M. Battaglia, and F. Mahmoudi, *Eur. Phys. J. C* **72**, 1906 (2012); A. Arbey, M. Battaglia, A. Djouadi, F. Mahmoudi, and J. Quevillon, *Phys. Lett. B* **708**, 162 (2012); S. Heinemeyer, O. Stal, and G. Weiglein, *Phys. Lett. B* **710**, 201 (2012); T. Li, J. A. Maxin, D. V. Nanopoulos, and J. W. Walker, *Phys. Lett. B* **710**, 207 (2012); J. Elias-Miro, J. R. Espinosa, G. F. Giudice, G. Isidori, A. Riotto, and A. Strumia, *Phys. Lett. B* **709**, 222 (2012); H. Baer, V. Barger, and A. Mustafayev, *Phys. Rev. D* **85**, 075010 (2012); C. Englert, T. Plehn, M. Rauch, D. Zerwas, and P. M. Zerwas, *Phys. Lett. B* **707**, 512 (2012); D. E. Kahana and S. H. Kahana, [arXiv:1112.2794](https://arxiv.org/abs/1112.2794); Z.-z. Xing, H. Zhang, and S. Zhou, *Phys. Rev. D* **86**, 013013 (2012); T. Moroi, R. Sato, and T. T. Yanagida, *Phys. Lett. B* **709**, 218 (2012); G. Guo, B. Ren, and X.-G. He, [arXiv:1112.3188](https://arxiv.org/abs/1112.3188); C. Cheung and Y. Nomura, *Phys. Rev. D* **86**, 015004 (2012); P. Draper, P. Meade, M. Reece, and D. Shih, *Phys. Rev. D* **85**, 095007 (2012); T. Moroi and K. Nakayama, *Phys. Lett. B* **710**, 159 (2012); P. M. Ferreira, R. Santos, M. Sher, and J. P. Silva, *Phys. Rev. D* **85**, 077703 (2012); A. Djouadi, O. Lebedev, Y. Mambrini, and J. Quevillon, *Phys. Lett. B* **709**, 65 (2012); M. Carena, S. Gori, N. R. Shah, and C. E. M. Wagner, *J. High Energy Phys.* **03** (2012) 014; M. Kadastik, K. Kannike, A. Racioppi, and M. Raidal, *J. High Energy Phys.* **05** (2012) 061; S. Akula, B. Altunkaynak, D. Feldman, P. Nath, and G. Peim, *Phys. Rev. D* **85**, 075001 (2012); O. Buchmueller, R. Cavanaugh, A. De Roeck, M. J. Dolan, J. R. Ellis, H. Flacher, S. Heinemeyer, G. Isidori *et al.*, *Eur. Phys. J. C* **72**, 2020 (2012); J. Cao, Z. Heng, D. Li, and J. M. Yang, *Phys. Lett. B* **710**, 665 (2012); C. Strece, G. Bertone, D. G. Cerdeno, M. Fornasa, R. R. de Austri, and R. Trotta, *J. Cosmol. Astropart. Phys.* **03** (2012) 030; G. Burdman, C. Haluch, and R. Matheus, *Phys. Rev. D* **85**, 095016 (2012); A. Arhrib, R. Benbrik, M. Chabab, G. Moulataka, and L. Rahili, *J. High Energy Phys.* **04** (2012) 136; A. Bottino, N. Fornengo, and S. Scopel, *Phys. Rev. D* **85**, 095013 (2012); L. J. Hall, D. Pinner, and J. T. Ruderman, *J. High Energy Phys.* **04** (2012) 131; A. Arvanitaki and G. Villadoro, *J. High Energy Phys.* **02** (2012) 144; U. Ellwanger, *J. High Energy Phys.* **03** (2012) 044; J. F. Gunion, Y. Jiang, and S. Kraml, *Phys. Lett. B* **710**, 454 (2012); S. F. King, M. Muhlleitner, and R. Nevzorov, *Nucl. Phys.* **B860**, 207 (2012); J. Cao, Z. Heng, J. M. Yang, Y. Zhang, and J. Zhu, *J. High Energy Phys.* **03** (2012) 086; L. Wang and X.-F. Han, [arXiv:1206.1673](https://arxiv.org/abs/1206.1673); A. Fowlie, M. Kazana, K. Kowalska, S. Munir, L. Roszkowski, E. M. Sessolo, S. Trojanowski, and Y.-L. S. Tsai, [arXiv:1206.0264](https://arxiv.org/abs/1206.0264).
- [4] A. Djouadi, *Phys. Rep.* **459**, 1 (2008).
- [5] P. Fayet, *Nucl. Phys.* **B90**, 104 (1975); *Phys. Lett.* **64B**, 159 (1976); **69B**, 489 (1977); **84B**, 416 (1979); H. P. Nilles, M. Srednicki, and D. Wyler, *Phys. Lett. B* **120**,

- 346 (1983); J.M. Frere, D.R. Jones, and S. Raby, *Nucl. Phys.* **B222**, 11 (1983); J.P. Derendinger and C.A. Savoy, *Nucl. Phys.* **B237**, 307 (1984); A.I. Veselov, M.I. Vysotsky, and K.A. Ter-Martirosian, *Sov. Phys. JETP* **63**, 489 (1986); J.R. Ellis, J.F. Gunion, H.E. Haber, L. Roszkowski, and F. Zwirner, *Phys. Rev. D* **39**, 844 (1989); M. Drees, *Int. J. Mod. Phys. A* **4**, 3635 (1989).
- [6] U. Ellwanger, M. Rausch de Traubenberg, and C.A. Savoy, *Phys. Lett. B* **315**, 331 (1993); *Z. Phys. C* **67**, 665 (1995); *Nucl. Phys.* **B492**, 21 (1997); U. Ellwanger, *Phys. Lett. B* **303**, 271 (1993); P. Pandita, *Z. Phys. C* **59**, 575 (1993); T. Elliott, S.F. King, and P.L. White, *Phys. Rev. D* **49**, 2435 (1994); S.F. King and P.L. White, *Phys. Rev. D* **52**, 4183 (1995); F. Franke and H. Fraas, *Int. J. Mod. Phys. A* **12**, 479 (1997).
- [7] D.J. Miller, R. Nevzorov, and P.M. Zerwas, *Nucl. Phys.* **B681**, 3 (2004).
- [8] U. Ellwanger, C. Hugonie, and A.M. Teixeira, *Phys. Rep.* **496**, 1 (2010); U. Ellwanger, *Eur. Phys. J. C* **71**, 1782 (2011).
- [9] S.F. King, M. Muhlleitner, and R. Nevzorov, *Nucl. Phys.* **B860**, 207 (2012).
- [10] S.F. King, S. Moretti, and R. Nevzorov, *Phys. Rev. D* **73**, 035009 (2006).
- [11] S.F. King, S. Moretti, and R. Nevzorov, *Phys. Lett. B* **634**, 278 (2006).
- [12] S.F. King, S. Moretti, and R. Nevzorov, *Phys. Lett. B* **650**, 57 (2007).
- [13] P. Athron, S.F. King, D.J. Miller, S. Moretti, and R. Nevzorov, *Phys. Rev. D* **80**, 035009 (2009).
- [14] P. Athron, S.F. King, D.J. Miller, S. Moretti, and R. Nevzorov, *Phys. Lett. B* **681**, 448 (2009).
- [15] P. Athron, S.F. King, D.J. Miller, S. Moretti, and R. Nevzorov, *Phys. Rev. D* **84**, 055006 (2011).
- [16] S.F. King, S. Moretti, and R. Nevzorov, [arXiv:hep-ph/0601269](https://arxiv.org/abs/hep-ph/0601269); S. Kraml *et al.*, Report No. CERN-2006-009, 2006 (unpublished); S.F. King, S. Moretti, and R. Nevzorov, *AIP Conf. Proc.* **881**, 138 (2007); R. Howl and S.F. King, *J. High Energy Phys.* **01** (2008) 030; P. Athron, S.F. King, D.J. Miller, S. Moretti, and R. Nevzorov, [arXiv:0810.0617](https://arxiv.org/abs/0810.0617).
- [17] R. Howl and S.F. King, *J. High Energy Phys.* **05** (2008) 008.
- [18] S.F. King, R. Luo, D.J. Miller, and R. Nevzorov, *J. High Energy Phys.* **12** (2008) 042.
- [19] J.P. Hall and S.F. King, *J. High Energy Phys.* **06** (2011) 006.
- [20] P.A. Kovalenko, R.B. Nevzorov, and K.A. Ter-Martirosian, *Yad. Fiz.* **61**, 898 (1998) [*Phys. At. Nucl.* **61**, 812 (1998)]; R.B. Nevzorov and M.A. Trusov, *Zh. Eksp. Teor. Fiz.* **91**, 1251 (2000) [*J. Exp. Theor. Phys.* **91**, 1079 (2000)]; R.B. Nevzorov, K.A. Ter-Martirosian, and M.A. Trusov, *Yad. Fiz.* **65**, 311 (2002) [*Phys. At. Nucl.* **65**, 285 (2002)].
- [21] C. Panagiotakopoulos and A. Pilaftsis, *Phys. Rev. D* **63**, 055003 (2001); D.J. Miller and R. Nevzorov, [arXiv:hep-ph/0309143](https://arxiv.org/abs/hep-ph/0309143); R. Nevzorov and D.J. Miller, *Proceedings to the 7th Workshop "What comes beyond the Standard Model,"* edited by N.S. Mankoc-Borstnik, H.B. Nielsen, C.D. Froggatt, and D. Lukman (DMFA-Zaloznistvo, Ljubljana, 2004), p. 107; D.J. Miller, S. Moretti, and R. Nevzorov, *Proceedings to the 18th International Workshop on High-Energy Physics and Quantum Field Theory (QFTHEP 2004)*, edited by M.N. Dubinin and V.I. Savrin (Moscow State Univ., Moscow, 2004) p. 212.
- [22] J. Rich, M. Spiro, and J. Lloyd-Owen, *Phys. Rep.* **151**, 239 (1987); P.F. Smith, *Contemp. Phys.* **29**, 159 (1988); T.K. Hemmick *et al.*, *Phys. Rev. D* **41**, 2074 (1990).
- [23] B.C. Allanach, *Comput. Phys. Commun.* **143**, 305 (2002).
- [24] S. Moretti and W.J. Stirling, *Phys. Lett. B* **347**, 291 (1995); **366**, 451(E) (1996).
- [25] Z. Kunszt, S. Moretti, and W.J. Stirling, *Z. Phys. C* **74**, 479 (1997).
- [26] The ATLAS Collaboration, Report No. ATLAS-CONF-2012-033.
- [27] The ATLAS Collaboration, Report No. ATLAS-CONF-2012-037.
- [28] The ATLAS Collaboration, Report No. ATLAS-CONF-2012-041.
- [29] The CMS Collaboration, Report No. CMS PAS SUS-12-005, 2012.
- [30] The CMS Collaboration, Report No. CMS PAS SUS-12-002, 2012.
- [31] T.J. LeCompte and S.P. Martin, *Phys. Rev. D* **84**, 015004 (2011).
- [32] G. Aad *et al.* (ATLAS Collaboration), *Phys. Rev. Lett.* **108**, 181802 (2012).
- [33] The ATLAS Collaboration, Report No. ATLAS-CONF-2012-036.
- [34] D. Alves *et al.* (LHC New Physics Working Group Collaboration), *J. Phys. G* **39**, 105005 (2012).
- [35] The CMS Collaboration, Report No. CMS PAS SUS-11-016, 2011; The CMS Collaboration, Report No. CMS PAS SUS-12-011, 2012.
- [36] The ATLAS Collaboration, Report No. ATLAS-CONF-2012-023.
- [37] G. Aad *et al.* (ATLAS Collaboration), *Phys. Rev. D* **83**, 112006 (2011).
- [38] S.L. Cheung, Report No. CERN-THESIS-2011-162.
- [39] R. Nevzorov, [arXiv:1205.5967](https://arxiv.org/abs/1205.5967).
- [40] The ATLAS Collaboration, Report No. ATLAS-CONF-2012-007.
- [41] The CMS Collaboration, Report No. CMS PAS EXO-11-019, 2011.
- [42] S. Chatrchyan *et al.* (CMS Collaboration), *Phys. Lett. B* **714**, 158 (2012).
- [43] E. Accomando, A. Belyaev, L. Fedeli, S.F. King, and C. Shepherd-Themistocleous, *Phys. Rev. D* **83**, 075012 (2011).
- [44] J. Kalinowski, S.F. King, and J.P. Roberts, *J. High Energy Phys.* **01** (2009) 066.
- [45] J.P. Hall and S.F. King, *J. High Energy Phys.* **08** (2009) 088.
- [46] J.P. Hall, S.F. King, R. Nevzorov, S. Pakvasa, and M. Sher, *Phys. Rev. D* **83**, 075013 (2011).
- [47] A. Belyaev, J.P. Hall, S.F. King, and P. Svantesson, *Phys. Rev. D* **86**, 031702 (2012).
- [48] S.F. King and A. Merle, *J. Cosmol. Astropart. Phys.* **08** (2012) 016.
- [49] F. Staub, *Comput. Phys. Commun.* **181**, 1077 (2010).
- [50] A. Pukhov, [arXiv:hep-ph/0412191](https://arxiv.org/abs/hep-ph/0412191).
- [51] P. Diessner, G. Hellwig, G.M. Pruna, D. Stockinegr, and A. Voigt (to be published).